Bioconjugate Chemistry

Communication

pubs.acs.org/bc

Engineered M13 Bacteriophage Nanocarriers for Intracellular Delivery of Exogenous Proteins to Human Prostate Cancer Cells

Sandra M. DePorter[†] and Brian R. McNaughton*[,†,‡]

[†]Department of Chemistry, and [‡]Department of Biochemistry & Molecular Biology, Colorado State University, Fort Collins, Colorado 80523, United States

Supporting Information

ABSTRACT: The size, well-defined structure, and relatively high folding energies of most proteins allow them to recognize disease-relevant receptors that present a challenge to small molecule reagents. While multiple challenges must be overcome in order to fully exploit the use of protein reagents in basic research and medicine, perhaps the greatest challenge is their intracellular delivery to a particular diseased cell. Here, we describe the genetic and enzymatic manipulation of prostate cancer cell-penetrating M13 bacteriophage to generate nanocarriers for the intracellular delivery of functional exogenous proteins to a human prostate cancer cell line.

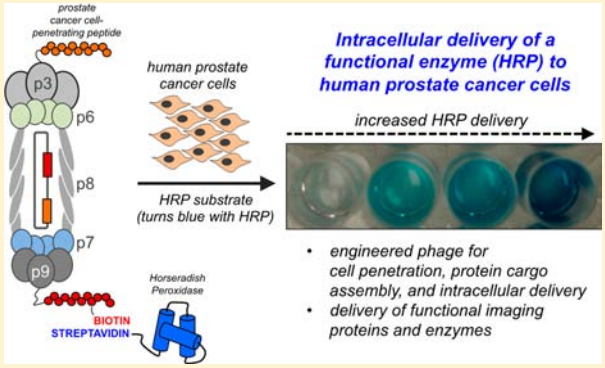

INTRODUCTION

Proteins represent a growing class of reagents in the global communities of basic research, pharmaceutical science, and biotechnology.[1,2] Proteins have unique features, which make them particularly useful for identifying and destroying diseased cells, and controlling disease-relevant cell function and fate. For example, potent enzymatic activity, in some proteins, allow researchers to image or alter cell function or fate through the use of a relatively small amount of material, compared to many small molecule reagents and drugs. Additionally, in contrast to small molecules, the size, relatively high folding energies, and well-defined structure of proteins often allow these reagents to potently and selectively recognize macromolecular surfaces that can confound small molecule discovery, such as protein−protein interactions.

While proteins have unique desirable characteristics, a number of barriers exist when considering their expanded use in basic and translational research. Perhaps foremost among these is the challenge of delivering functional protein reagents to the interior of a diseased cell. Unlike most traditional small molecule reagents and drugs, the majority of natural and synthetic proteins are not able to penetrate the lipid bilayer membrane of mammalian cells. This largely limits the functional utility of protein reagents and drugs to those that target cell surface receptors. In response to this challenge, significant effort and resources have been dedicated to the development of technologies for intracellular delivery of exogenous proteins. These generally include: microinjection,[3] liposomes,[4] lipid-linked proteins,[5] nanoparticles,[6] fusions to receptor ligands,[7] polyarginine[8] and arginine grafting,[9] supercharged proteins,[10−13] and protein transduction domains (cell-penetrating peptides).[14] Most often, targeted delivery of protein cargo to a diseased cell relies on antibody fusions and conjugates.[15] However, native antibodies, and their fragments, generally do not actively deliver fused or conjugated cargo to the interior of a targeted cell, and only localize cargo to the cell surface. Typically, appreciable internalization of antibodies and their fragments is only achieved by fusion to a transduction domain.[16,17] Additionally, conjugation or genetic fusion to a transduction domain only permits internalization of a single protein per transduction event, resulting in relatively low efficiency of functional cargo delivery.

The encapsulation of multiple protein reagents within a polymeric nanoparticle or liposome can enable the delivery of relatively large payloads of exogenous protein cargo to the interior of a cell. However, these technologies often require multiple synthetic and purification steps, which generally involve covalent attachment of cell-targeting and/or cell-penetration components, and incorporation of components that improve pharmacokinetic properties (such as evasion from the innate immune response). Additionally, precise chemical control over the composition, rigidity, size, and shape of the nanomaterial scaffold is needed, since relatively small changes to these features can result in dramatically different biodistribution, biocompatibility, and function.[18−20] Finally, encapsulation of the protein reagent(s) and functional display of the targeting and/or cell-penetrating reagents must be finely orchestrated, largely by means of chemical synthesis.

An alternative approach is to use a genetically defined nanomaterial with spatially defined exterior components that can be selectively altered through genetic or enzymatic

Received: May 29, 2014
Published: August 18, 2014

   dx.doi.org/10.1021/bc500339k | *Bioconjugate Chem.* 2014, 25, 1620−1625

manipulation. This approach largely overcomes challenges faced by chemical construction and selective manipulation of synthetic nanomaterials. If multiple copies of protein cargo can be selectively complexed or attached, relatively large payload delivery per transduction event can be achieved. M13 filamentous bacteriophage (referred to as phage herein) are a well-studied nanomaterial with a width of ~6 nm and length of ~930 nm.[21] Phage is composed of 5 coat proteins, 4 minor coat proteins (p3, p6, p7, and p9) and a major coat protein p8, which encapsulate a ssDNA genome (Figure 1A). These

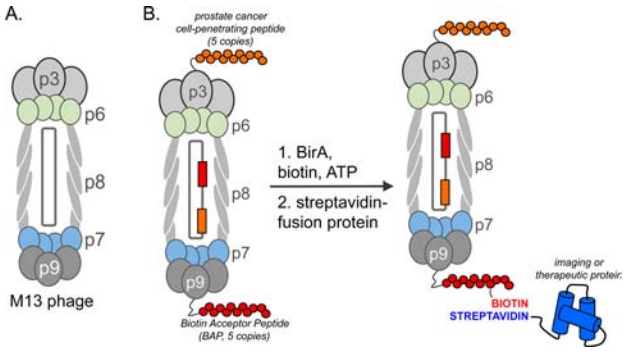

Figure 1. (A) M13 phage with major and minor coat proteins labeled. (B) Strategy for the construction of M13 phage nanocarriers for intracellular delivery of a functional imaging or therapeutic protein to human prostate cancer cells. Phage are genetically engineered to display a prostate cancer cell-penetrating peptide on the N-terminus of phage coat protein 3 (p3) and a biotin acceptor peptide (BAP) on the N-terminus of phage coat protein 9 (p9). Following purification of the phage by standard methods from *E. coli*, they were site-selectively biotinylated with biotin ligase (BirA) and incubated with a fusion protein that consists of streptavidin and an exogenous protein for delivery. This results in stably assembled phage that contain the cell-penetrating component on p3 and exogenous protein on p9.

nanorods exhibit properties that are desirable for use as reagents in basic and translational research. The ssDNA genome of M13 phage can be manipulated with relative ease, enabling the construction of engineered phage that selectively display spatially defined foreign peptides and/or proteins with unique and desirable properties.[22,23] In addition, phage can be evolved for a variety of desired functions, which include cell recognition and penetration. Finally, phage can be modified with polyethylene glycol (PEG),[24] or genetically modified to display a "self" peptide,[25] potentially allowing modified phage to evade the human immune system. These virtues have been not been overlooked by researchers, and phage have been used to deliver a wide range of reagents to the exterior or interior of mammalian cells including DNA,[26−28] small molecules,[29−32] nanoparticles,[33] and peptides.[34] Janda and co-workers have reported the use of engineered bacteriophage that display cocaine-sequestering antibodies, which remove circulating cocaine.[35,36]

While phage coat protein 3 can be genetically modified to display foreign peptides or proteins of varied size and structure, genetic fusion of large peptides (>12 amino acids) or proteins to coat proteins p6, p7, p8, and p9 often results in very low display efficiency (or no display). For example, genetic fusion to major coat protein p8 requires the use of both a phagemid to encode a displayed protein on p8 and helper phage to encode all other phage proteins that make the phage infect *E. coli* and replicate.[37] This process typically yields a heterogeneous population of phage that may display as few as one foreign protein. Genetic fusion to minor coat proteins p7 and p9 requires separation of overlapping gene regions and the introduction of a signal sequence in order to display proteins and peptides larger than approximately 15 amino acids.[38] While phage can be engineered for improved display,[39] higher efficiencies are highly dependent on the composition and size of the foreign peptide or protein. Here, we describe a strategy that relies on genetic and enzymatic manipulation of phage, and in vitro assembly, to generate phage nanoreagents that display a potent human prostate cancer cell-penetrating peptide on p3, and controllably assemble with a recombinant fusion protein to display relatively large payloads of exogenous protein on p9 (Figure 1B).

We recently reported phage that potently and selectively penetrate PC-3 human prostate cancer cells in complex solutions containing human blood.[40] Prostate cancer cell recognition and penetration is achieved by virtue of a 12 amino acid peptide (YTFGLKTSFNVQ), termed Ypep, which is genetically fused to the N-terminus of p3. More recently, we described mutagenesis efforts resulting in a T7A mutant of Ypep (termed Ypep2, herein) which exhibits dramatically improved prostate cancer cell-selectivity and cell-penetration efficiencies.[41] When Ypep2 is fused to the N-terminus of p3 on phage, dramatically improved potency of phage uptake is observed in PC-3 cells, compared to phage that display Ypep. Interestingly, the potency and selectivity of phage cell-penetration is dictated by multivalency effects. While protein cargo fused to a single Ypep (or variant thereof) actively penetrate cells, transduction is appreciably less potent and cell-selective compared to phage that bear ~5 copies of Ypep (or variants thereof) as a fusion to p3. Given the excellent cell-penetrating potency and cell-selectivity of these phage, we questioned whether they could be engineered as nanocarriers for intracellular delivery of exogenous protein cargo to prostate cancer cells.

RESULTS AND DISCUSSION

We genetically modified phage to display Ypep2 prostate cancer cell-penetrating peptide on the N-terminus of p3, and the biotin acceptor peptide (termed BAP, GLNDIFEAQKIEWHE) on the N-terminus of p9 (Ypep2(p3)/BAP(p9)). This phage was then biotinylated in vitro by incubation with *E. coli* BirA (Supporting Information). To assess the feasibility of this complexation strategy, we separately expressed and purified a streptavidin-Green Fluorescent Protein fusion protein (SAV-GFP), which was then incubated with biotinylated phage. Phage were precipitated twice with PEG/NaCl and washed to remove any SAV-GFP that remained in the supernatant. These phage are herein referred to as Ypep2(p3)/SAV-GFP(p9). SAV-GFP assembly was confirmed by Western blot (Figure 2A) and fluorescence analysis of the phage pellet, which appears bright green (Figure 2B). PC-3 cells were treated with a solution containing $\sim 1 \times 10^{10}$ pfu/ml or $\sim 1.6 \times 10^{-11}$ M Ypep2(p3)/SAV-GFP(p9).

To determine the number of SAV-GFP fusion proteins that are complexed to each phage, we prepared phage that display a FLAG peptide tag (DYKDDDDK) on the N-terminus of p3 and BAP on p9. These phage were biotinylated, then complexed with a SAV-GFP fusion bearing a FLAG tag. The relative levels of p3-FLAG and SAV-GFP-FLAG were measured by Western blot. Based on densitometry ratios over 3 separate experiments, on average we estimated that each phage contains

dx.doi.org/10.1021/bc500339k | *Bioconjugate Chem.* 2014, 25, 1620−1625

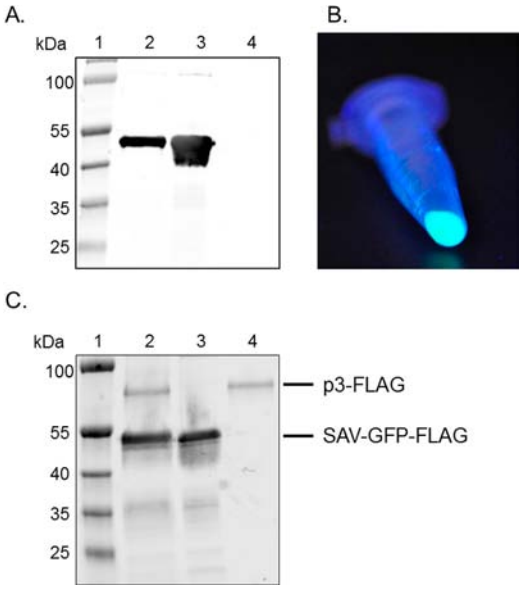

Figure 2. (A) Western blot, showing: (lane 1) ladder; (lane 2) Ypep2(p3)/SAV-GFP(p9) phage; (lane 3) purified recombinant SAV-GFP; and (lane 4) supernatant from final precipitation of Ypep2(p3)/SAV-GFP(p9) phage. The expected molecular weight of the SAV-GFP fusion is ~44.3 kDa. (B) Phage that display prostate cancer cell-penetrating component (Ypep-2) on the N-terminus of p3, and biotin acceptor peptide (BAP) on the N-terminus of p9, following in vitro biotinylation with BirA and assembly with streptavidin-Green Fluorescent Protein (SAV-GFP) and washing/pelleting. Phage are illuminated with a long wave (365 nm) hand-held lamp. (C) Western blot of FLAG(p3)/SAV-GFP-FLAG(p9) phage. The membrane was treated with an Abcam anti-FLAG primary antibody and visualized with a LI-COR goat anti-rabbit IR dye 800 CW secondary antibody.

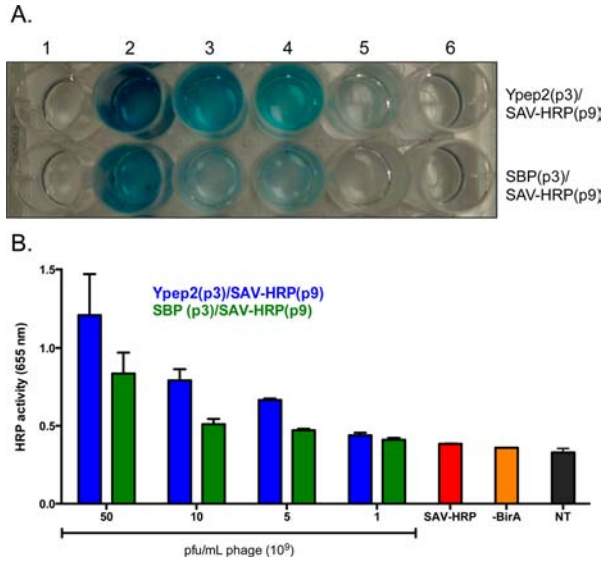

Figure 3. (A) Image of a multiwell plate that contain a monolayer of PC-3 cells, following: (lane 1) no treatment; (lane 2) 50×10^9; (lane 3) 10×10^9; (lane 4) 5×10^9; (lane 5) 1×10^9 Ypep2(p3)/SAV-HRP(p9) or SBP(p3)/SAV-HRP(p9) pfu/mL phage; or (lane 6) ~1.6 nM (based on SAV concentration) recombinant SAV-HRP. (B) Quantitated data from the image shown in (A). Blue bars = HRP activity in cells, following treatment with Ypep2(p3)/SAV-HRP(p9); green bars = HRP activity in cells, following treatment with SBP(p3)/SAV-HRP(p9); red bars = HRP activity in cells, following treatment with ~1.6 nM SAV-HRP; orange bar = HRP activity in cells, following treatment with phage that were not biotinylated prior to incubation with SAV-HRP; NT = no treatment. Error bars represent the standard deviation of two separate experiments.

approximately 4 copies of SAV-GFP-FLAG per copy of p3-FLAG (Figure 2C). Since streptavidin is a homotetramer, and approximately the same number of copies of p3 and p9 are displayed on phage, these findings suggest that each copy of p9 is biotinylated and complexed to an SAV-GFP-FLAG tetramer. Thus, at least in the case of GFP, each phage carries ~20 copies of the cargo protein (which is fused to SAV).

Expanding on these findings, we tested the delivery of a functional enzyme using our phage nanocarrier strategy. We focused on the intracellular delivery of horseradish peroxidase (HRP), which enjoys broad use in bioimaging, and has therapeutic utility. Assembly of SAV-HRP to biotinylated phage, and robust HRP enzymatic activity of the resulting reagent (Ypep2(p3)/SAV-HRP(p9)) was verified by incubating this phage with a known HRP substrate (3,3′,5,5′-tetramethylbenzidine, TMB). While Ypep2(p3)/SAV-HRP(p9) phage act on TMB, resulting in a colorimetric reaction, supernatant taken after washes to pellet the phage does not contain measurable levels of HRP (Supporting Information, Figure S1). These findings support a model wherein SAV-HRP assembles with biotinylated phage to generate enzymatically active nanorods. PC-3 cells were treated with solutions that contain ~50×10^9 to 1×10^9 pfu/mL (~8.3×10^{-11} to 1.6×10^{-12} M) Ypep2(p3)/SAV-HRP(p9) phage, and washed to remove cell surface-bound material. Impressively, cells treated with the three highest concentrations of phage were found to have appreciable levels of intracellular HRP, as determined by colorimetric analysis (Figure 3A, top row). These data are shown in Figure 3B, blue bars. In contrast, cells treated with ~1.6×10^{-9} M SAV-HRP (Figure 3B, red bar) were not found to contain appreciable levels of intracellular HRP. As a control, phage that display Ypep2 on p3 and BAP on p9 (but not biotinylated with BirA) were incubated with SAV-HRP, and phage were precipitated and washed as before. When PC-3 were treated with these phage, no appreciable HRP activity was observed (Figure 3B, orange bar). These data indicate that assembly of SAV-HRP to biotinylated phage is required for phage-dependent delivery of the pendant protein cargo.

To assess the relative cell-penetrating and functional enzyme delivery efficiencies of Ypep2(p3)/HRP(p9) phage, we compared them to analogous phage that do not display Ypep2, but display a recently reported cancer cell homing/cell-penetrating peptide (SPPTGIN) that binds to the matricellular protein SPARC (secreted protein, acidic, cysteine-rich).[42] Overexpression of SPARC has been associated with a number of cancers, including prostate cancer. SPARC binding peptide (SBP) was previously used by Belcher and co-workers for phage-dependent delivery of iron oxide nanoparticles to PC-3 cells (which express appreciable levels of SPARC).[43] We constructed the SBP(p3)/SAV-HRP(p9) and measured HRP uptake following incubation with PC-3 cells with solutions containing ~50×10^9 to 1×10^9 pfu/mL (~8.3×10^{-11} to 1.6×10^{-12} M) SBP(p3)/SAV-HRP(p9) phage (Figure 3A, bottom row, and Figure 3B, green bars). Phage that display Ypep2 generally deliver significantly more HRP to PC-3 cells, compared to analogous phage that contain SBP in place of Ypep2. Treatment with a solution containing ~50 or ~10×10^9 pfu/mL of Ypep2(p3)/HRP(p9) phage were found to have

dx.doi.org/10.1021/bc500339k | Bioconjugate Chem. 2014, 25, 1620−1625

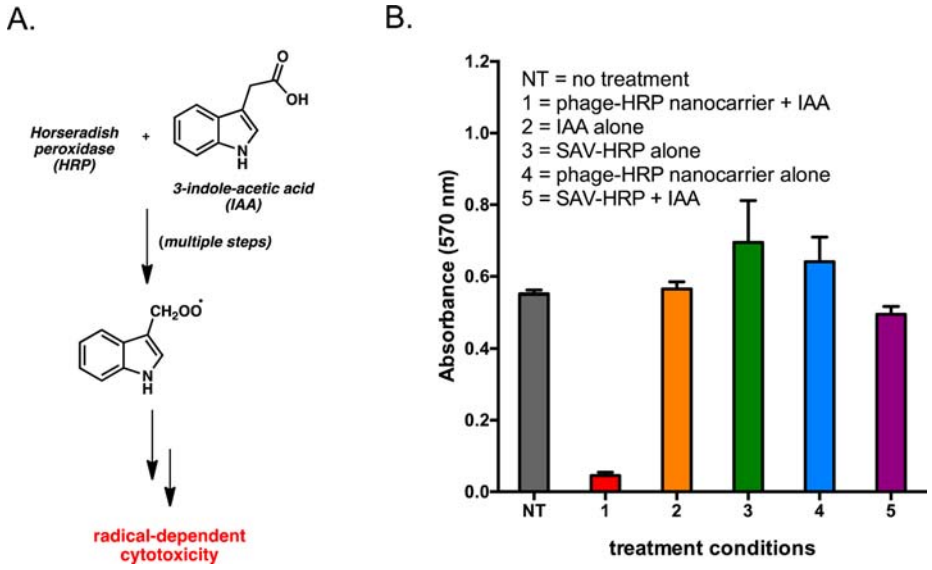

Figure 4. (A) HRP-dependent oxidation of indole-3-acetic acid (IAA) produces a peroxyl radical, which leads to toxicity in mammalian cells. (B) Cell toxicity (as determined by an MTT assay) as a result of concomitant IAA treatment and intracellular delivery of HRP to PC-3 cells, via the phage nanocarriers. Error bars represent the standard deviation of two separate experiments.

~1.5-fold higher levels of HRP, compared to cells treated with the identical concentrations of the SBP-displayed variant.

The ability of HRP to act on colorimetric and fluorescent substrates, including reagents that emit in the far-red (which is useful for deep tissue imaging), is well documented. Additionally, HRP can act on pro-drug substrates, and thus, intracellular HRP and concomitant treatment of these substrates can lead to cell death. The plant hormone indole-3-acetic acid (IAA) is a prodrug that is acted on by HRP to form a peroxyl radical, which ultimately leads to radical-dependent cytotoxicity and cell death (Figure 4A).[44−46] To measure the functional utility of phage nanocarriers as delivery reagents of a therapeutic enzyme, we treated PC-3 cells with 6 mM IAA and ~5×10^{10} pfu/mL (~8.3×10^{-12} M) Ypep2(p3)/HRP(p9) phage. Following treatment, we assayed cytotoxicity using a commercially available thiazolyl blue tetrazolium bromide (MTT) cell viability assay. As shown in Figure 4B (red bar), we observed virtually complete cell death, following treatment with both Ypep2(p3)/HRP(p9) phage and IAA, compared to untreated cells (Figure 4B, gray bar). In contrast, no appreciable toxicity was observed in cells following treatment with either 6 mM IAA (Figure 4B, orange bar) or ~1.6×10^{-8} M SAV-HRP, which is ~4 orders of magnitude more HRP than used in the phage-assisted delivery experiment (Figure 4B, green bar), or ~5×10^{10} pfu/mL Ypep2(p3)/HRP(p9) phage (Figure 4B, blue bar). Treatment with both 6 mM IAA and ~1.6×10^{-8} M SAV-HRP does not result in appreciable cell death (Figure 4B, purple bar). Thus, functional levels of SAV-HRP does not accumulate in the cell interior (via transduction), but HRP delivery (and subsequent action on IAA) is facilitated by Ypep2(p3)/HRP(p9) phage nanocarriers.

CONCLUSION

This Communication describes our efforts to engineer M13 bacteriophage as genetically defined nanorod materials for the delivery of relatively large payloads of exogenous functional proteins to mammalian cells (PC-3 cells in this study). Phage are equipped with a prostate cancer cell-penetrating reagent on p3, and complexed with approximately 4 copies of a streptavidin-fusion protein or conjugate on p9. Concomitant treatment with Ypep2(p3)/HRP(p9) phage and the pro-drug IAA results in appreciable cell death, demonstrating that phage-assisted delivery of HRP has therapeutic utility. Throughout, our strategy relies on genetic modification of phage coat proteins 3 and 9 (p3 and p9, respectively), such that p3 displays a potent PC-3 cell-penetrating peptide (Ypep2), and p9 displays a biotin-acceptor peptide. Following in vitro biotinylation with *E. coli* biotin ligase (BirA), these phage are assembled with protein cargo that is either genetically fused, or conjugated, to streptavidin, which tightly binds biotin. Previously, we have shown that phage bearing ~5 copies of Ypep-derived peptides on the N-terminus of p3 potently penetrate PC-3 cells, in complex solutions. Here, we show that genetic and enzymatic manipulation of these phage, and decoration with exogenous protein assemblies on p9, leads to potent delivery of this protein cargo to PC-3 cells. This strategy is modular. Various previously reported cell-penetrating reagents can be incorporated by genetic engineering, and diverse streptavidin−protein fusions and conjugates can easily be used. Since the phage genome predetermines the size and spatial localization of components that make up this nanomaterial, phage can be genetically or enzymatically manipulated selectively. This approach overcomes some of the challenges associated with strategies that rely on the chemical synthesis and manipulation of synthetic nanocarriers for exogenous protein delivery.

ASSOCIATED CONTENT

Supporting Information

Detailed experimental methods and additional data. This material is available free of charge via the Internet at http://pubs.acs.org.

AUTHOR INFORMATION

Corresponding Author

*E-mail: brian.mcnaughton@colostate.edu.

Notes

The authors declare no competing financial interest.

■ ACKNOWLEDGMENTS

The authors gratefully acknowledge funding from a DoD-CDMRP Prostate Cancer Research Program New Investigator Award and Colorado State University Cancer Supercluster. S.M.D. is a recipient of the Alfred R. Bader Award for Student Innovation in synthetic organic chemistry and chemical biology, sponsored by Sigma-Aldrich.

■ REFERENCES

(1) Carter, P. J. (2011) Introduction to current and future protein therapeutics: a protein engineering perspective. *Exp. Cell Res. 317*, 1261−9.
(2) Leader, B., Baca, Q. J., and Golan, D. E. (2008) Protein therapeutics: a summary and pharmacological classification. *Nat. Rev. Drug Discovery 7*, 21−39.
(3) Feramisco, J. R., Gross, M., Kamata, T., Rosenberg, M., and Sweet, R. W. (1984) Microinjection of the oncogene form of the human H-ras (T-24) protein results in rapid proliferation of quiescent cells. *Cell 38*, 109−17.
(4) Gregoriadis, G. (1995) Engineering liposomes for drug delivery: progress and problems. *Trends Biotechnol. 13*, 527−37.
(5) Zelphati, O., Wang, Y., Kitada, S., Reed, J. C., Felgner, P. L., and Corbeil, J. (2001) Intracellular delivery of proteins with a new lipid-mediated delivery system. *J. Biol. Chem. 276*, 35103−10.
(6) Utama, R. H., Guo, Y., Zetterlund, P. B., and Stenzel, M. H. (2012) Synthesis of hollow polymeric nanoparticles for protein delivery via inverse miniemulsion periphery RAFT polymerization. *Chem. Commun. 48*, 11103−5.
(7) Gabel, C. A., and Foster, S. A. (1986) Mannose 6-phosphate receptor-mediated endocytosis of acid hydrolases: internalization of beta-glucuronidase is accompanied by a limited dephosphorylation. *J. Cell Biol. 103*, 1817−27.
(8) Fuchs, S. M., and Raines, R. T. (2005) Polyarginine as a multifunctional fusion tag. *Protein Sci. 14*, 1538−44.
(9) Fuchs, S. M., and Raines, R. T. (2007) Arginine grafting to endow cell permeability. *ACS Chem. Biol. 2*, 167−70.
(10) Cronican, J. J., Beier, K. T., Davis, T. N., Tseng, J. C., Li, W., Thompson, D. B., Shih, A. F., May, E. M., Cepko, C. L., Kung, A. L., Zhou, Q., and Liu, D. R. (2011) A class of human proteins that deliver functional proteins into mammalian cells in vitro and in vivo. *Chem. Biol. 18*, 833−8.
(11) Cronican, J. J., Thompson, D. B., Beier, K. T., McNaughton, B. R., Cepko, C. L., and Liu, D. R. (2010) Potent delivery of functional proteins into Mammalian cells in vitro and in vivo using a supercharged protein. *ACS Chem. Biol. 5*, 747−52.
(12) McNaughton, B. R., Cronican, J. J., Thompson, D. B., and Liu, D. R. (2009) Mammalian cell penetration, siRNA transfection, and DNA transfection by supercharged proteins. *Proc. Natl. Acad. Sci. U.S.A. 106*, 6111−6.
(13) Thompson, D. B., Cronican, J. J., and Liu, D. R. (2012) Engineering and identifying supercharged proteins for macromolecule delivery into mammalian cells. *Methods Enzymol. 503*, 293−319.
(14) Deshayes, S., Morris, M. C., Divita, G., and Heitz, F. (2005) Cell-penetrating peptides: tools for intracellular delivery of therapeutics. *Cell. Mol. Life Sci. 62*, 1839−49.
(15) Teicher, B. A., and Chari, R. V. (2011) Antibody conjugate therapeutics: challenges and potential. *Clin. Cancer Res. 17*, 6389−97.
(16) Niesner, U., Halin, C., Lozzi, L., Gunthert, M., Neri, P., Wunderli-Allenspach, H., Zardi, L., and Neri, D. (2002) Quantitation of the tumor-targeting properties of antibody fragments conjugated to cell-permeating HIV-1 TAT peptides. *Bioconjugate Chem. 13*, 729−36.
(17) Muller, S., Zhao, Y., Brown, T. L., Morgan, A. C., and Kohler, H. (2005) TransMabs: cell-penetrating antibodies, the next generation. *Expert Opin. Biol. Ther. 5*, 237−41.
(18) Alexis, F., Pridgen, E., Molnar, L. K., and Farokhzad, O. C. (2008) Factors affecting the clearance and biodistribution of polymeric nanoparticles. *Mol. Pharmaceutics 5*, 505−15.
(19) He, C., Hu, Y., Yin, L., Tang, C., and Yin, C. (2010) Effects of particle size and surface charge on cellular uptake and biodistribution of polymeric nanoparticles. *Biomaterials 31*, 3657−66.
(20) Merkel, T. J., Chen, K., Jones, S. W., Pandya, A. A., Tian, S. M., Napier, M. E., Zamboni, W. E., and DeSimone, J. M. (2012) The effect of particle size on the biodistribution of low-modulus hydrogel PRINT particles. *J. Controlled Release 162*, 37−44.
(21) Wang, Y. A., Yu, X., Overman, S., Tsuboi, M., Thomas, G. J., and Egelman, E. H. (2006) The structure of a filamentous bacteriophage. *J. Mol. Biol. 361*, 209−215.
(22) Smith, G. P. (1985) Filamentous fusion phage - novel expression vectors that display cloned antigens on the virion surface. *Science 228*, 1315−1317.
(23) Smith, G. P., and Petrenko, V. A. (1997) Phage display. *Chem. Rev. 97*, 391−410.
(24) Kim, K. P., Cha, J. D., Jang, E. H., Klumpp, J., Hagens, S., Hardt, W. D., Lee, K. Y., and Loessner, M. J. (2008) PEGylation of bacteriophages increases blood circulation time and reduces T-helper type 1 immune response. *Microb. Biotechnol. 1*, 247−57.
(25) Rodriguez, P. L., Harada, T., Christian, D. A., Pantano, D. A., Tsai, R. K., and Discher, D. E. (2013) Minimal "Self" peptides that inhibit phagocytic clearance and enhance delivery of nanoparticles. *Science 339*, 971−5.
(26) Larocca, D., Burg, M. A., Jensen-Pergakes, K., Ravey, E. P., Gonzalez, A. M., and Baird, A. (2002) Evolving phage vectors for cell targeted gene delivery. *Curr. Pharm. Biotechnol. 3*, 45−57.
(27) Dunn, I. S. (1996) Mammalian cell binding and transfection mediated by surface-modified bacteriophage lambda. *Biochimie 78*, 856−61.
(28) Poul, M. A., and Marks, J. D. (1999) Targeted gene delivery to mammalian cells by filamentous bacteriophage. *J. Mol. Biol. 288*, 203−11.
(29) Vaks, L., and Benhar, I. (2011) In vivo characteristics of targeted drug-carrying filamentous bacteriophage nanomedicines. *J. Nanobiotechnol. 9*, 58.
(30) Suthiwangcharoen, N., Li, T., Li, K., Thompson, P., You, S. J., and Wang, Q. (2011) M13 bacteriophage-polymer nanoassemblies as drug delivery vehicles. *Nano. Res. 4*, 483−493.
(31) Li, K., Chen, Y., Li, S. Q., Huong, G. N., Niu, Z. W., You, S. J., Mello, C. M., Lu, X. B., and Wang, Q. A. (2010) Chemical modification of M13 bacteriophage and its application in cancer cell imaging. *Bioconjugate Chem. 21*, 1369−1377.
(32) Bar, H., Yacoby, I., and Benhar, I. (2008) Killing cancer cells by targeted drug-carrying phage nanomedicines. *BMC Biotechnol. 8*, DOI: 10.1186/1472-6750-8-37.
(33) Ghosh, D., Lee, Y., Thomas, S., Kohli, A. G., Yun, D. S., Belcher, A. M., and Kelly, K. A. (2012) M13-templated magnetic nanoparticles for targeted in vivo imaging of prostate cancer. *Nat. Nanotechnol. 7*, 677−682.
(34) Ivanenkov, V. V., and Menon, A. G. (2000) Peptide-mediated transcytosis of phage display vectors in MDCK cells. *Biochem. Biophys. Res. Commun. 276*, 251−257.
(35) Dickerson, T. J., Kaufmann, G. F., and Janda, K. D. (2005) Bacteriophage-mediated protein delivery into the central nervous system and its application in immunopharmacotherapy. *Expert Opin. Biol. Ther. 5*, 773−781.
(36) Carrera, M. R. A., Kaufmann, G. F., Mee, J. M., Meijler, M. M., Koob, G. F., and Janda, K. D. (2004) Treating cocaine addiction with viruses. *Proc. Natl. Acad. Sci. U.S.A. 101*, 10416−10421.
(37) Rakonjac, J., Jovanovic, G., and Model, P. (1997) Filamentous phage infection-mediated gene expression: construction and propagation of the gIII deletion mutant helper phage R408d3. *Gene 198*, 99−103.
(38) Ghosh, D., Kohli, A. G., Moser, F., Endy, D., and Belcher, A. M. (2012) Refactored M13 bacteriophage as a platform for tumor cell imaging and drug delivery. *ACS Synth. Biol. 1*, 576−582.
(39) Sidhu, S. S., Feld, B. K., and Weiss, G. A. (2007) M13 bacteriophage coat proteins engineered for improved phage display. *Methods Mol. Biol. 352*, 205−19.

(40) DePorter, S. M., Lui, I., Mohan, U., and McNaughton, B. R. (2013) A protein transduction domain with cell uptake and selectivity profiles that are controlled by multivalency effects. *Chem. Biol. 20*, 434−444.
(41) DePorter, S. M., Lui, I., Bruce, V. J., Gray, M. A., Lopez-Islas, M., and McNaughton, B. R. (2014) Mutagenesis modulates the uptake efficiency, cell-selectivity, and functional enzyme delivery of a protein transduction domain. *Mol. Biosyst. 10*, 18−23.
(42) Smith, B. A., Daniels, D. S., Coplin, A. E., Jordan, G. E., McGregor, L. M., and Schepartz, A. (2008) Minimally cationic cell-permeable miniature proteins via alpha-helical arginine display. *J. Am. Chem. Soc. 130*, 2948−2949.
(43) Kelly, K. A., Waterman, P., and Weissleder, R. (2006) In vivo imaging of molecularly targeted phage. *Neoplasia 8*, 1011−8.
(44) Kim, D. S., Jeon, S. E., and Park, K. C. (2004) Oxidation of indole-3-acetic acid by horseradish peroxidase induces apoptosis in G361 human melanoma cells. *Cell. Signalling 16*, 81−8.
(45) Wardman, P. (2002) Indole-3-acetic acids and horseradish peroxidase: a new prodrug/enzyme combination for targeted cancer therapy. *Curr. Pharm. Des. 8*, 1363−74.
(46) Yan, M., Du, J., Gu, Z., Liang, M., Hu, Y., Zhang, W., Priceman, S., Wu, L., Zhou, Z. H., Liu, Z., Segura, T., Tang, Y., and Lu, Y. (2010) A novel intracellular protein delivery platform based on single-protein nanocapsules. *Nat. Nanotechnol. 5*, 48−53.